to the transient nature of the 4a-OH adduct and the slower rates of their turnovers versus rat liver PAH. For each enzyme, every hydroxylation event involves the formation of the 4a-OH adduct, a situation entirely analogous to PAH.

It is especially interesting to note that the copper-containing PAH appears to follow the same mechanism of oxygen activation as do the iron enzymes. The greater ease of obtaining resolved ESR spectra with the Cu^{2+} form of the bacterial enzyme prompted us to examine the proximity of the metal ion center to the pterin cofactor. ESR spectra of the enzyme recorded in the presence of [5-^{14}N]6,7-dimethyltetrahydropterin or [5-^{15}N]6,7-dimethyltetrahydropterin were computer simulated and found to be consistent with the pterin serving as a direct donor ligand to the copper center through the N-5 position. Presuming that the pyrazine ring–metal interaction is maintained upon reduction of the cupric ion to the active cuprous form, this study provides support for the underlying assumption of close proximity between the metal center and the pterin implicit in the mechanism depicted in Figure 3.[70]

The mechanistic links between PAH and the other aromatic amino acid hydroxylases provide a rationale for the enzymes sharing the common pathway of oxygen activation outlined above. Some differences do exist, as demonstrated by comparing TH with PAH. Although phenylalanine is the more difficult substrate to hydroxylate, PAH has a V_{max} about 100 times greater than that of TH. Conversely, PAH autoinactivates during turnover whereas TH does not. These facts do not obviously correlate with a commonality of oxygen activation. One possible explanation of the above differences may be the degree to which each enzyme must use its ferrous center to activate oxygen. As mentioned above, structural and energy considerations predict the 4a-OOH adduct to be close to a peracid in oxygen-transferring ability. Peracids are capable of hydroxylating tyrosine but not phenylalanine in aqueous media. Thus TH may hydroxylate simply by providing a passive environment for the generation of 4a-OOH adduct in the proximity of its substrate. With PAH, additional oxygen activation is needed, which is provided by the interaction of the 4a-OOH adduct with the ferrous center. The consequence of this interaction with PAH is the possibility of ferrous-induced homolytic cleavage of the 4a-OOH adduct's oxygen–oxygen bond, resulting in the generation of hydroxyl radicals, which play a part in enzyme inactivation. Thus PAH, which may simply be an "evolved" TH, may be less stable due to its requirement for generating a more potent hydroxylating intermediate.

(70) Pember, S. O.; Benkovic, S. J.; Villafranca, J. J.; Pasenkiewicz-Gierula, M.; Antholine, W. E. *Biochemistry* **1987**, *26*, 4483.

Registry No. PAH, 9029-73-6; O_2, 7782-44-7; Fe, 7439-89-6; monooxygenase, 9038-14-6; tetrahydropterin, 1008-35-1.

EPR Studies of Long-Range Intramolecular Electron–Electron Exchange Interaction

GARETH R. EATON*

Department of Chemistry, University of Denver, Denver, Colorado 80208

SANDRA S. EATON

Department of Chemistry, University of Colorado—Denver, Denver, Colorado 80204

Received July 28, 1987 (Revised Manuscript Received November 16, 1987)

If asked to name long-range interaction phenomena in chemical systems, many chemists would probably cite electron transfer, fluorescence resonance energy transfer, or perhaps NMR coupling. Electron–electron exchange interactions, in contrast, would likely be identified as short range. The fact that exchange interaction between two paramagnetic centers is often not recognized as a long-range phenomenon is largely a function of the techniques that have typically been used to study it. Electron–electron exchange has been studied by magnetic susceptibility measurements in which interactions weaker than kT are too small to detect. Since interaction that is strong enough to be observed by magnetic susceptibility typically occurs only between unpaired electrons that are separated by a few angstroms, the impression has evolved that electron–electron exchange interaction is a short-range phenomenon. When collisions between paramagnetic molecules in solution give rise to exchange, the strongest interaction is during the time of closest approach, which again emphasizes the short-range terms. In the EPR spectra of solids with high concentrations of unpaired electrons, exchange-narrowing also requires close proximity of the paramagnetic centers.

Gareth R. Eaton was born in Lockport, NY, in 1940 and received his A.B. from Harvard College in 1962. He served in the U.S. Navy, assigned to the AEC, from 1962 to 1967. He received his Ph.D. in inorganic chemistry from MIT in 1972. He is currently Professor of Chemistry and Dean of Natural Sciences at the University of Denver.

Sandra S. Eaton was born in Boston, MA, in 1946 and received her B.A. from Wellesley College in 1968. She received her Ph.D. in inorganic chemistry from MIT in 1972. She is currently Professor of Chemistry at the University of Colorado—Denver.

0001-4842/88/0121-0107$01.50/0

In NMR, nuclear spin exchange interaction results in spin–spin coupling. The characteristic multiplet patterns in proton NMR spectra are familiar to most chemists. Electron–nuclear exchange gives rise to nuclear hyperfine splitting in EPR spectra and is used to identify the nuclei in the vicinity of an unpaired electron. Since the electron magnetic moment is 658 times larger than the nuclear magnetic moment and since long-range nuclear couplings have been observed, it seemed reasonable to us to expect that EPR would provide a method to examine electron–electron interactions that are weaker than those that can be studied by magnetic susceptibility.

This report concerns our determinations of electron–electron exchange interactions by EPR. Although the first recognition of electron–electron spin–spin splitting in EPR was in spectra of nitroxyl diradicals[1,2] and vanadyl tartrate dimers,[3,4] we have chosen to examine primarily systems in which the two interacting unpaired electrons are nonequivalent—one unpaired electron is on a transition metal and the second unpaired electron is on a nitroxyl radical. These centers were selected to provide synthetic flexibility and to afford products that are sufficiently stable that they can be isolated and characterized. Due to their stability, nitroxyl radicals have been widely used as "spin labels". The nitroxyl unpaired electron is primarily in the N–O π^* orbital. Since the separation between the metal and nitroxyl electron spin energy levels is a function of the metal g value and the nuclear hyperfine splitting of the metal EPR spectrum, variation of the metal in the spin-labeled metal complex provides a wide range of energy-level separations.

In this Account we first describe the analysis of EPR spectra that exhibit resolved electron–electron coupling. This is followed by a discussion of the relationship between the coupling constant J and electron spin delocalization. Finally, we provide examples of chemical information that can be obtained from studies of electron–electron coupling.

Effect of Intramolecular Electron–Electron Exchange on EPR Spectra

Electron–electron spin–spin interaction causes splitting of the energy levels for the two unpaired electrons, analogous to nuclear spin–spin splitting in NMR spectra. However, the EPR spectra often appear more complicated than the AX, AM, or AB patterns that are readily recognized in NMR spectra because there are nuclear spins that are coupled to the electron spins and electron–nuclear and electron–electron coupling can be of the same order of magnitude. Just as in NMR, these patterns can be analyzed by considering subspectra. The electron–electron spin–spin coupling constant is designated as J. The fluid solution splitting pattern is independent of the sign of J.

The EPR spectrum of vanadyl bis(hexafluoroacetylacetonate), $VO(hfac)_2$, in fluid solution consists of eight lines due to hyperfine splitting by the vanadium nuclear spin ($I = {}^7/_2$). There are three lines in the EPR spectrum of a nitroxyl radical due to hyperfine splitting

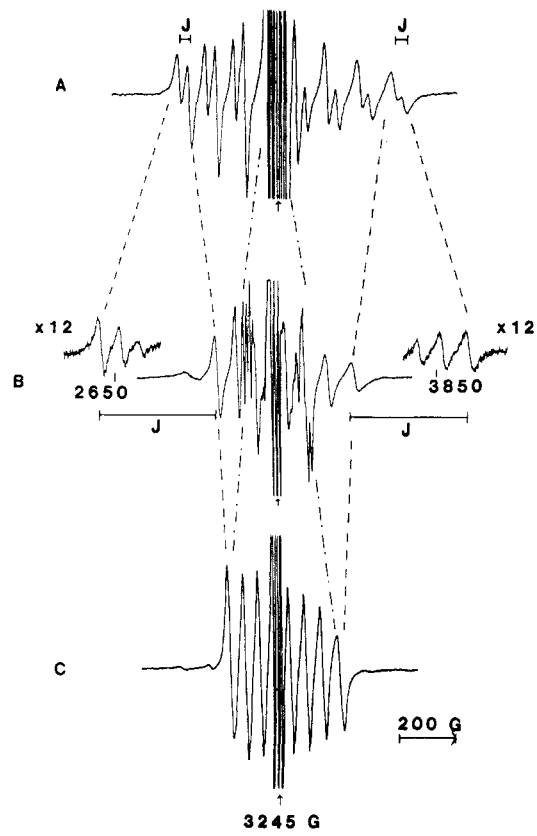

Figure 1. X-band (9.10 GHz) EPR spectra in solution at room temperature for $VO(hfac)_2$·I (A), $VO(hfac)_2$·II (B), and $VO(hfac)_2$·III (C). The lines indicate the changes in the positions of the nitroxyl (–·–) and vanadyl (– – –) lines as a function of J for the AB patterns resulting from interaction of the vanadyl $m_i = \pm{}^7/_2$ transitions with the nitroxyl. The sharp three-line spectrum that is off-scale is due to a small amount of spin-labeled pyridine that is not bound to $VO(hfac)_2$. The signals for the coordinated nitroxyl are also off-scale in spectrum A.

by the nitrogen nuclear spin ($I = 1$). Figure 1A shows the EPR spectrum that was obtained when spin-labeled pyridine I[5] was bound to $VO(hfac)_2$ via the pyridine

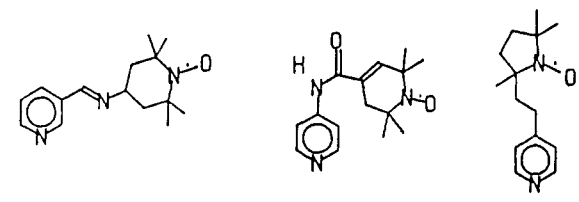

I II III

nitrogen, forming a 1:1 complex. Each of the eight vanadium lines is split into a doublet by the coupling to the nitroxyl unpaired electron. The doublet splitting is equal to the electron–electron coupling constant, J (36 G). One doublet of vanadium lines is obscured by the nitroxyl signals in the center of the spectrum. Similarly, each of the lines in the nitroxyl spectrum is split into a doublet. The electron–electron coupling constant in this complex is small relative to the differences between the energy levels for the vanadyl and nitroxyl unpaired electrons and the spectrum is analogous to an AX NMR spectrum. When J is this small the vanadyl hyperfine splitting is the same as observed in the absence of interaction with the nitroxyl.

When discussing spectra in which the value of J is comparable to the electron spin energy level differences,

(1) Briere, P.; Dupeyre, R.-M.; Lemaire, H.; Morat, C.; Rassat, A.; Rey, P. *Bull. Chim. Soc. Fr.* **1965**, 3290.
(2) Glarum, S. H.; Marshall, J. H. *J. Chem. Phys.* **1976**, *47*, 1374.
(3) Dunhill, R. H.; Symons, M. C. R. *Mol. Phys.* **1968**, *15*, 105.
(4) James, P. G.; Luckhurst, G. R. *Mol. Phys.* **1970**, *18*, 141.
(5) Sawant, B. M.; Shroyer, A. L. W.; Eaton, G. R.; Eaton, S. S. *Inorg. Chem.* **1982**, *21*, 1093.

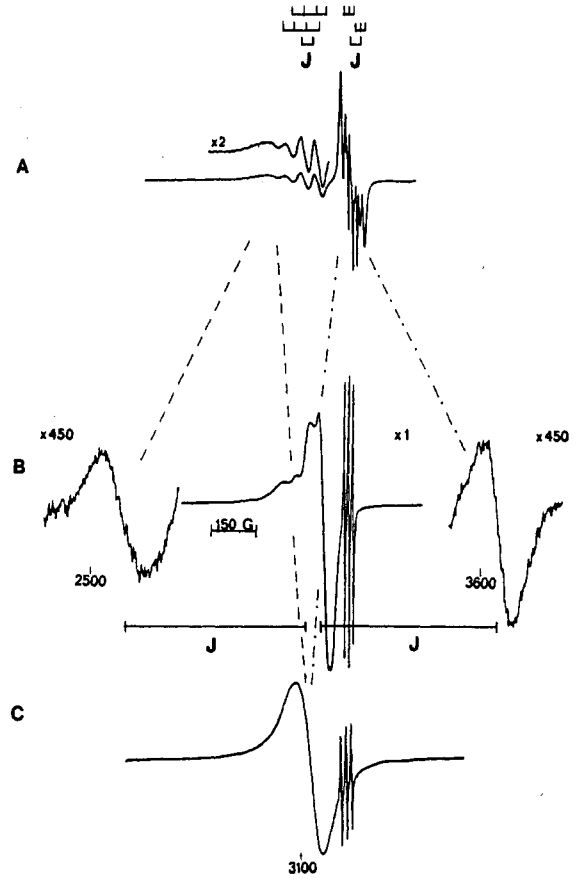

Figure 2. X-band (9.10 GHz) EPR spectra in solution at room temperature for $Cu(hfac)_2$·IV (A), $Cu(hfac)_2$·V (B), and $Cu(hfac)_2$·VI (C). The lines indicate the changes in the positions of the nitroxyl (-·-) and copper (---) lines as the value of J increases.

it is convenient to use nomenclature analogous to that which is used for NMR AB spectra.[6] Thus we refer to the "outer" and "inner" lines of the AB splitting patterns. The interaction causes mixing of the metal and nitroxyl wave functions, so designation of lines as "metal" or "nitroxyl" indicates the nature of the transitions in the limit of weak interaction.

The EPR spectrum of the complex $VO(hfac)_2$·II[5] in dichloromethane solution is shown in Figure 1B. The value of J in this spectrum (425 G) is about 10 times as large as for the spectrum in Figure 1A (36 G). There is an AB pattern for each combination of a vanadyl nuclear spin state and a nitroxyl nitrogen nuclear spin state or $8 \times 3 = 24$ AB patterns. However, the nitroxyl nitrogen hyperfine splitting is too small to be resolved for most of the transitions so the spectrum can be viewed as eight AB patterns. The correspondence between the positions of the transitions for two of the AX patterns in Figure 1A and the related AB patterns in Figure 1B is indicated by the dashed lines in Figure 1. On going from Figure 1A to 1B the vanadyl and nitroxyl inner lines move closer together and the outer lines move away from the center of the spectrum. The vanadyl outer lines are centered at 2650 G for the AB patterns involving the vanadyl lines that occur at lower field than the nitroxyl in the absence of spin–spin interaction and at 3850 G for the vanadyl lines that occur at higher field than the nitroxyl. The lowest and highest field vanadyl outer lines are more intense than the other vanadyl outer lines because the separation between the vanadyl and nitroxyl energy levels is greater for the highest and lowest field vanadyl lines than for other combinations of vanadyl and nitroxyl lines. In this spectrum the nitroxyl outer lines are obscured by more intense transitions.

As the value of J becomes large relative to the separation between the nitroxyl and vanadyl electron spin energy levels, the vanadyl and nitroxyl inner lines merge to an "averaged" spectrum and the intensity of the outer lines goes to zero. The spectrum of $VO(hfac)_2$·III[7] in Figure 1C is an example of J large enough to give an averaged spectrum. The g value is the average of that for vanadyl and nitroxyl, and the vanadyl nuclear hyperfine splitting is half that observed in the absence of electron–electron spin–spin interaction. The nitroxyl nitrogen hyperfine splitting on each of the eight lines is not resolved, but is also reduced to half of the value observed in the absence of electron–electron spin–spin interaction.

Figure 2 demonstrates the effect of increasing values of J on the EPR spectra for three spin-labeled pyridines bound to copper bis(hexafluoroacetylacetonate), $Cu(hfac)_2$. The EPR spectrum of $Cu(hfac)_2$ is split into four lines due to hyperfine splitting by the copper nuclear spin ($I = {}^3/_2$). In the spectrum of $Cu(hfac)_2$·IV[8] (Figure 2A), the magnitude of J (44 G) is comparable

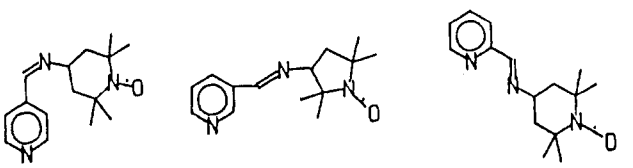

IV V VI

to the nuclear hyperfine splittings, and the EPR spectrum is approximately a doublet of quartets for the copper lines and a doublet of triplets for the nitroxyl lines. The difference between the copper and nitroxyl g values is sufficiently large that all of the copper lines occur to low field of the nitroxyl lines. In the spectrum of $Cu(hfac)_2$·V[9] (Figure 2B), the value of J (490 G) is about 10 times as large as for the spectrum in Figure 2A. The outer lines in Figure 2B are shifted away from the center of the spectrum and have decreased intensity. The copper transitions are at lower field than the nitroxyl lines, so all of the copper outer lines contribute to the signal at 2500 G, and all of the nitroxyl outer lines contribute to the signal at 3600 G. The nuclear hyperfine splitting of the outer lines was not resolved due to the large line widths of the signals. The inner copper and nitroxyl lines are closer together in Figure 2B than in Figure 2A, and the copper nuclear hyperfine splitting is partially resolved. In the spectrum of $Cu(hfac)_2$·VI[8] (Figure 2C), the value of J is >1000 G, which is sufficiently large to give an averaged spectrum.

The spectra in Figures 1 and 2 were obtained in fluid solution, so molecular tumbling was sufficiently rapid to average out anisotropic contributions to the electron–electron spin–spin splitting, and only the exchange

(6) Drago, R. S., Ed. *Physical Methods in Chemistry*; Saunders: Philadelphia, 1977; pp 270–277.

(7) More, K. M.; Eaton, G. R.; Eaton, S. S.; Hideg, K., to be published.

(8) Boymel, P. M.; Eaton, G. R.; Eaton, S. S. *Inorg. Chem.* **1980**, *19*, 727.

(9) Boymel, P. M.; Braden, G. A.; Eaton, G. R.; Eaton, S. S. *Inorg. Chem.* **1980**, *19*, 735.

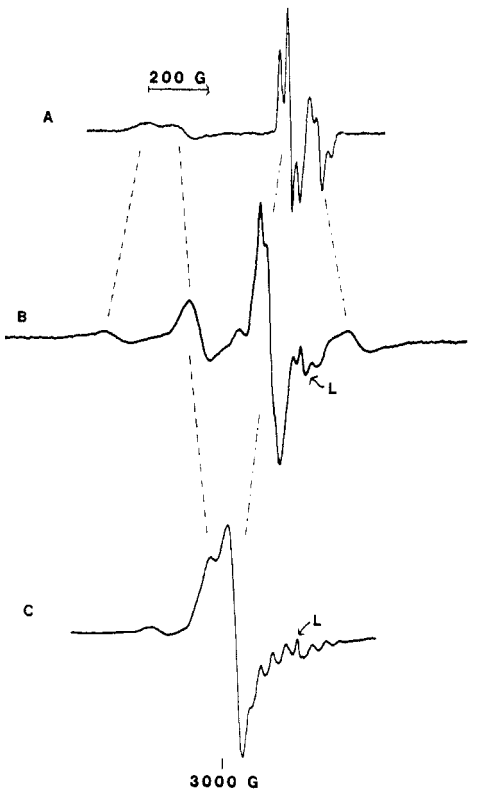

Figure 3. X-band (9.10 GHz) EPR spectra in frozen solution at −180 °C for Co(P)·IV (A), Co(P)·II (B), and Co(P)·VII (C). The lines indicate the changes in the positions of the nitroxyl (-·-) and cobalt perpendicular lines (---) as the value of J increases. L denotes the signal for spin-labeled ligand that is not bound to Co(P). The dipolar contribution to the spin–spin splitting is approximately the same for the three spectra in this figure with a maximum in each case of <30 G along the interspin vector.

contribution was observed. In rigid lattices (frozen solutions, powders, or large molecules that are not tumbling rapidly in solution) there is also an anisotropic through-space dipole–dipole contribution to the electron–electron coupling. This contribution is inversely proportional to r^3, where r is the distance between the two paramagnetic centers. The separation of these two contributions is discussed in detail in ref 10. When the exchange contribution is greater than the dipolar contribution and the dipolar term is approximately constant, increasing values of J cause collapse of AB patterns in frozen solution, analogous to what is observed in fluid solution. An illustration is presented in Figure 3. The prominent features in frozen-solution EPR spectra are the transitions that occur at the "extrema" or "turning points" of the distribution of orientation-dependent transitions.

When pyridine binds to cobalt(II) *p*-(trifluoromethyl)tetraphenylporphyrin (Co(P)), the resulting complex contains low-spin Co(II) with one unpaired electron. The EPR spectrum of Co(P)·py in frozen solution at 9.1 GHz has a large peak at about 2800 G that does not show resolved hyperfine splitting (the perpendicular lines) and a weaker eight-line signal at 3200 G (the parallel lines) with cobalt nuclear hyperfine splitting ($I = {}^7/_2$) of about 80 G. In the spectrum of Co(P)·IV[11] (Figure 3A) the pair of peaks at about 2800 G is due to splitting of the cobalt perpendicular lines by electron–electron spin–spin interaction with the nitroxyl. The nitroxyl signal at higher field is also split into a doublet. The cobalt parallel lines are obscured by the nitroxyl signals.

Comparison of the spectrum of Co(P)·II[11] (Figure 3B) with that in Figure 3A shows the changes that occur as the value of J increases. As in fluid solution, the cobalt and nitroxyl outer lines move away from the center of the spectrum and lose intensity and the inner lines move closer together. The spectrum of Co(P)·VII[7] (Figure 3C) is an example of an averaged spectrum. In

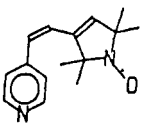

VII

this spectrum the parallel lines are observed with hyperfine splitting of about 40 G, which is half of that observed in the absence of electron–electron spin–spin interaction.

There are two key points to be learned from the examination of the spectra in Figures 1–3. (1) The AB patterns in EPR spectra due to exchange interaction between two unpaired electrons can be analyzed by analogy with NMR AB patterns. Although the treatment of the spectra in this Account is qualitative, quantitative computer simulations, including dipole and exchange terms can be performed. Details of computer simulation of electron–electron spin–spin splitting in fluid solution[12] and frozen solution[11,13] have been reported. The analysis has been extended to metals with more than one unpaired electron.[14,15] (2) The electron–electron exchange interaction is observable over relatively large numbers of bonds. The interaction for Cu(hfac)$_2$·VI was through 5 bonds. The interaction in the other complexes discussed above was through 8–10 bonds. Resolved AB splittings have been observed at distances as long as about 20 Å.[16]

Correspondence between the Value of J and Electron Spin Delocalization

Since exchange interaction is due to overlap of delocalized orbitals containing the unpaired electrons, the value of J is expected to correlate with other measures of electron spin delocalization. This expectation has been confirmed in a variety of systems.

When Ag(II), Cu(II), and VO(IV) were coordinated to spin-labeled porphyrins VIII and IX, the values of J decreased in the order Ag(II) > Cu(II) > VO(IV).[17] The hyperfine splitting in the EPR spectra of metalloporphyrins due to interaction of the unpaired electron with the nuclear spins of the coordinated nitrogens is an indication of the extent of delocalization of the unpaired electron into the porphyrin orbitals. The ni-

(10) Eaton, G. R.; Eaton, S. S., accepted for publication in *Spin Labeling III*.
(11) Eaton, S. S.; Boymel, P. M.; Sawant, B. M.; More, J. K.; Eaton, G. R. *J. Magn. Reson.* **1984**, *56*, 183.
(12) Eaton, S. S.; DuBois, D. L.; Eaton, G. R. *J. Magn. Reson.* **1978**, *32*, 251.
(13) Eaton, S. S.; More, K. M.; Sawant, B. M.; Boymel, P. M.; Eaton, G. R. *J. Magn. Reson.* **1983**, *52*, 435.
(14) More, K. M.; Eaton, G. R.; Eaton, S. S.; Hideg, K. *Inorg. Chem.* **1986**, *25*, 3865.
(15) More, K. M.; Eaton, G. R.; Eaton, S. S. *Inorg. Chem.* **1986**, *25*, 2638.
(16) Kokorin, A. I.; Novozhilova, G. A.; Shapiro, A. B. *Izv. Akad. Nauk, SSSR Khim.* **1981**, 286 (p 215 in translation).
(17) More, K. M.; Eaton, S. S.; Eaton, G. R. *J. Am. Chem. Soc.* **1981**, *103*, 1087.

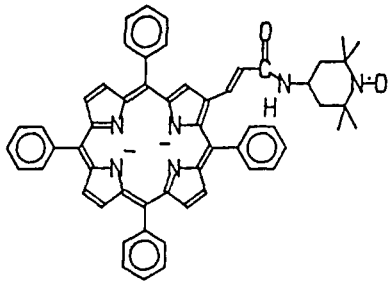

cis isomer VIII

trans isomer IX

trogen hyperfine splitting for M(tetraphenylporphyrin), M(TPP), also decreases in the order Ag(II) > Cu(II) > VO(IV).[18] ENDOR measurements of the interaction between the transition metal and the protons on the porphyrin ring also indicate that spin delocalization decreases in the order Ag(II) > Cu(II) > VO(IV).[19] Thus the trend in the values of J for these complexes parallels two other measures of the extent of electron spin delocalization. The spin delocalization of the metal unpaired electron into the porphyrin orbitals has a large contribution from σ orbitals. Comparison of the values of J for complexes of VIII and IX and an analogous spin-labeled porphyrin with a saturated linkage indicated that the values of J decreased in the order trans olefin > saturated $(CH_2)_2$ hydrocarbon > cis olefin.[17,20] This order does not correlate with π bonding. Instead it parallels observations that long-range electron–proton coupling in saturated hydrocarbons is dependent on the geometry of the chain and is greatest for systems with a "W-plan" geometry[21] as in IX. Thus the dependence of the values of J on the porphyrin–nitroxyl linkage indicates that delocalization in these complexes has more σ character than π character.

Values of J have been obtained for a series of spin-labeled pyridines, including I–VII, bound to Cu(hfac)$_2$,[5,8,9] Co(P),[11] VO(hfac)$_2$,[5] and Cr(TPP)Cl.[7,14,22] In the pyridine adducts of Cu(hfac)$_2$ the pyridine is in the basal plane of a square pyramid, and the Cu(II) unpaired electron is in the $d_{x^2-y^2}$ orbital, which has σ symmetry with respect to the orbitals on the pyridine nitrogen.[5] Pyridine binds axially to Co(P), and the Co(II) unpaired electron is in the d_{z^2} orbital, which thus has σ symmetry with respect to the orbital on the pyridine nitrogen.[11] Similar values of J were observed when the same spin-labeled pyridine was coordinated to Cu(hfac)$_2$ or to Co(P), which is consistent with the expected similarity in the spin delocalization mechanism for the two systems. In these complexes the substantial σ contribution to the spin delocalization caused values of J to be similar for the 3- and 4-isomers of the spin-labeled pyridines.

Pyridine binds cis to the V=O bond in VO(hfac)$_2$, and the vanadyl unpaired electron is in the d_{xy} orbital, which has π symmetry with respect to the orbitals on the pyridine nitrogen.[5] Pyridine binds axially to Cr(TPP)Cl, and the Cr(III) unpaired electrons are in the d_{xz} and d_{yz} orbitals, which have π symmetry with respect to the orbitals on the pyridine nitrogen.[14] The patterns in the values of J were similar for the VO(hfac)$_2$ and Cr(TPP)Cl complexes, and the value of J was substantially larger for the 4-isomers than for the 3-isomers of the spin-labeled ligands, consistent with a substantial π contribution to the spin delocalization.

As expected for a through-bond interaction, exchange is dependent on the linkage between the pyridine and the spin label. The value of J decreases in the order Schiff base > urea > amide > ester,[20] which parallels the order of decreasing π contribution to the bonding in the linkage. When a CH_2 group is added to the linkage between the pyridine and the nitroxyl, the value of J decreases by a factor of 100–200 for a urea linkage and decreases by a factor of 5–50 for amide linkages. Thus the effect of the CH_2 group is greater for linkages with large π contributions to the spin delocalization than for linkages with little π delocalization.

If the geometry of a metal–nitroxyl complex is held constant and the electron–electron interaction involves a single half-filled orbital on the metal, the value of J is expected to be proportional to $1/n$, where n is the number of unpaired electrons on the metal.[23] The value of n cannot be varied experimentally without altering other properties of the metal that may contribute to changes in the value of J. The spin-labeled pyridine complexes with VO(hfac)$_2$ (n = 1) and Cr(TPP)Cl (n = 3) provide comparisons for two first-row transition metals. The values of J for the Cr(III) complexes were $^1/_2$ to $^2/_3$ of the values observed for the vanadyl complexes,[14] which is a larger ratio than the $^1/_3$ expected if n were the only parameter that had been varied. The lower oxidation state of chromium in Cr(TPP)Cl than of vanadium in VO(tfac)$_2$ may cause a greater spin delocalization of the chromium unpaired electrons than of the vanadyl unpaired electron. Furthermore, although the geometry of the metalloporphyrin complex is fairly rigidly defined, the geometry of the vanadyl complex may be distorted, thereby decreasing the effectiveness of the overlap between the vanadyl and pyridine orbitals.

Rotated single-crystal EPR data have been obtained for the Cu(II)[24] and Ag(II)[25] complexes of spin-labeled porphyrins VIII and IX and the vanadyl complex of VIII.[26] Several conformations of the complexes were observed in the crystal. These conformations had different values of J and different distances, r, between the two paramagnetic centers. There was no correlation between the values of r and J, which is consistent with the expectation that the exchange interaction is determined by orbital overlap and does not have a simple functional dependence on the distance between the two unpaired electrons.

Applications to Chemical Problems

Since electron–electron spin–spin interaction provides distinctive EPR spectra and since the coupling constants are sensitive to changes in molecular geometry and coordination, the EPR spectra of spin-coupled systems can provide chemical information that would be difficult to obtain by other techniques. Examples

(18) Lin, W. C. In *The Porphyrins*; Dolphin, D., Ed.; Academic: New York, 1979; Vol. IVB, pp 355–377.
(19) Brown, T. G.; Hoffman, B. M. *Mol. Phys.* **1980**, *39*, 1073.
(20) More, K. M.; Eaton, G. R.; Eaton, S. S. *Can. J. Chem.* **1982**, *60*, 1392.
(21) King, F. W. *Chem. Rev.* **1976**, *76*, 157.
(22) Eaton, S. S.; Eaton, G. R. *Coord. Chem. Rev.*, in press.
(23) Hay, P. J.; Thibeault, J. C.; Hoffmann, R. *J. Am. Chem. Soc.* **1975**, *97*, 4884.
(24) Damoder, R.; More, K. M.; Eaton, G. R.; Eaton, S. S. *J. Am. Chem. Soc.* **1983**, *105*, 2147.
(25) Damoder, R.; More, K. M.; Eaton, G. R.; Eaton, S. S. *Inorg. Chem.* **1983**, *22*, 3738.
(26) Damoder, R.; More, K. M.; Eaton, G. R.; Eaton, S. S. *Inorg. Chem.* **1983**, *22*, 2836.

are given below for studies of weak orbital overlap, kinetics, and equilibria.

Weak Orbital Overlap. An important question in areas as diverse as electron transport, fluorescence resonance energy transfer, and NMR coupling is the significance of weak orbital overlaps that are sometimes called "through-space" interactions. These are not interactions through the primary bonding pathways. Rather, these are interactions due to spatial proximity of orbitals on atoms that are not bonded to (i.e., adjacent to, in an HMO sense) each other. When such orbital overlaps permit spin–spin interaction between two paramagnetic centers, the result is stronger exchange coupling than would have been expected through the primary bonding pathway.

EPR spectra of the copper(II) complexes of spin-labeled porphyrins X and XI have been examined in

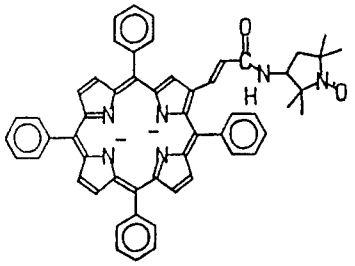

cis isomer X

trans isomer XI

several solvents.[27] The values of J for the trans isomer, XI, were 3–5 G. The values of J for the cis isomer were 5–10 G in solvents that coordinate to the copper (tetrahydrofuran and pyridine), but increased to 550 G in chloroform solution. The cis olefinic linkage positions the substituent above the porphyrin plane while the trans olefin positions the substituent beside the porphyrin plane. It was proposed therefore that in the absence of a coordinating solvent, there was a weak orbital overlap between the amide oxygen in the cis isomer and the copper orbitals or the porphyrin π orbitals and that coordination of solvent to the copper caused conformational changes that prevented the weak orbital overlap.

Similarly, a series of copper(II) tetraphenylporphyrins has been studied in which a spin label is attached to one phenyl ring. The values of J in fluid solution were several orders of magnitude greater when the substituent was attached to the ortho position of the phenyl ring than when the substituent was attached to the meta or para positions.[28] The values of J were strongly solvent dependent for the ortho isomers, but not for the meta or para isomers. These results indicate that there was a pathway for spin–spin interaction that was only accessible to the ortho isomers, presumably involving direct interaction of orbitals from the substituent with the metalloporphyrin orbitals. For a silver(II) complex of an ortho-spin-labeled porphyrin, the values of J in solutions of noncoordinating solvents were about 1000 G and dropped to about 100 G in pyridine solution.[29] In frozen solution the EPR spectra indicated that the increase in J was accompanied by about a 2-Å decrease in the silver–nitroxyl distance. Thus the increase in the value of J in noncoordinating solvents was attributed to a conformational change that increased the interaction between the side-chain orbitals and the metalloporphyrin orbitals.

Crystal structures of first-row transition-metal complexes of bis(pyrazolyl)amines, XII, have shown that the

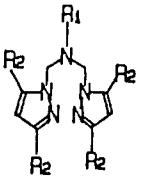

XII

complexes can adopt a range of conformations ranging from no bonding interaction between the metal and the central amine nitrogen to metal–amine nitrogen distances of 2.12–2.19 Å.[30] EPR spectra at 9 GHz of $Cu(XII)X_2$ with X = Cl, Br, R_1 = nitroxyl, and R_2 = H showed an averaged spectrum. At 35 GHz the larger energy-level separation resulted in an AB spectrum from which a value of J = 2000 G was obtained. In $Cu(XII)X_2$, X = Cl, Br, R_1 = nitroxyl, and R_2 = CH_3, the values of J were 50–800 G and were strongly dependent on solvent and temperature, which indicates that the change of R_2 from H to CH_3 caused a weakening of the bond between the copper and amine nitrogen. The resulting conformation was quite flexible and was subject to variation as a function of solvent and temperature.

Kinetics. Electron–electron spin–spin interaction is sufficiently strong in $Cu(XIII)_2$ to give an averaged spectrum. Since there are two nitroxyl radicals interacting with the copper, the copper nuclear hyperfine splitting in the averaged spectrum is one-third of that in $Cu(XIV)_2$.[31] Cu(XIII)(XIV) is formed by ligand

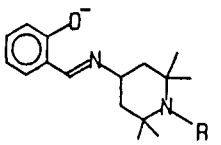

R = O XIII

R = H XIV

exchange between $Cu(XIII)_2$ and $Cu(XIV)_2$ and has a copper nuclear hyperfine splitting one-half of that in $Cu(XIV)_2$. Rates of ligand exchange were obtained by monitoring the EPR spectra in toluene solution as a function of time. The process is associative and the second-order rate constant is about 20 M^{-1} min^{-1}, which is much slower than is typically observed for ligand exchange of Cu(II) complexes in aqueous solution.

Coordination Equilibria. The EPR spectra of XV (n = 2, 3) showed the presence of two isomers with populations that were solvent and temperature dependent.[32,33] The values of J for XV, n = 2, in toluene

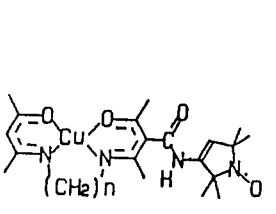

XV

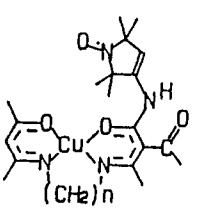

XVI

(27) More, K. M.; Eaton, S. S.; Eaton, G. R. *Inorg. Chem.* **1981**, *20*, 2641.

(28) More, K. M.; Sawant, B. M.; Eaton, G. R.; Eaton, S. S. *Inorg. Chem.* **1981**, *20*, 3354.

(29) More, K. M.; Eaton, G. R.; Eaton, S. S. *Inorg. Chem.* **1984**, *23*, 4084.

(30) Reibenspies, J. H.; Anderson, O. P.; Eaton, S. S.; More, K. M.; Eaton, G. R. *Inorg. Chem.* **1987**, *26*, 132 and references therein.

(31) Eaton, S. S.; Eaton, G. R. *Inorg. Nucl. Chem. Lett.* **1979**, *15*, 29.

(32) Eaton, S. S.; More, K. M.; DuBois, D. L.; Boymel, P. M.; Eaton, G. R. *J. Magn. Reson.* **1980**, *41*, 150.

solution at room temperature were 510 G (55%) and 3135 G (45%). At 9 GHz the intensities of the outer lines of the AB patterns with J = 3135 G were so small that the lines were difficult to detect. At 35 GHz the separation between the copper and nitroxyl electron spin energy levels was increased, which increased the intensities of the outer lines and facilitated their detection. On the basis of the differences in the values of J and the similarities in the IR spectra for the two isomers, the isomer with the larger value of J was assigned as XVI. This type of isomerization had been proposed previously, but had not been detected by other spectroscopic methods.

In the EPR spectra of $VO(tfac)_2(py{\sim}NO)$ (py~NO is a spin-labeled pyridine and tfac = trifluoroacetylacetonate), two isomers were observed with values of J that differed by about 20%, although only a single isomer was observed when the same spin-labeled pyridines were bound to $VO(hfac)_2$.[5] A larger difference in the values of J would be expected if the isomerism were due to coordination of the pyridine nitrogen cis and trans to the V=O bond. Since the isomers were observed with the unsymmetrically substituted tfac and not with the symmetrically substituted hfac, the isomers are assigned to coordination of the spin-labeled ligand trans to the two different ends of the β-diketonate as sketched in XVII and XVIII.

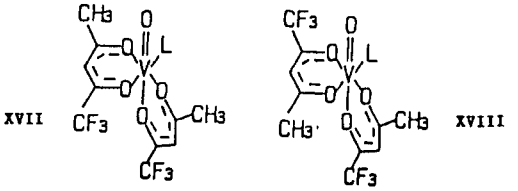

(33) DuBois, D. L.; Eaton, G. R.; Eaton, S. S. *J. Am. Chem. Soc.* **1979**, *101*, 2624.

Concluding Remarks

Electron–electron exchange interaction causes AB splittings in EPR spectra. Numerous examples have been obtained for interaction through 8–12 bonds and up to 14 Å. Electron–electron spin–spin exchange is a sufficiently long-range phenomenon that one should not assume a purely dipolar interaction model for any system unless the exchange contribution has been demonstrated not to be significant. The dependence of the magnitude of electron–electron exchange interaction on molecular structure and bonding compels interpretation in terms of orbital overlap. Thus, values of the coupling constant J are measures of the extent of electron spin delocalization. As we learn more about the efficiency of electron–electron exchange through various bonding pathways, the magnitude of J can be used to probe the orbital structure of complex molecules and to analyze conformational changes.

The recognition that exchange can extend through numerous bonds has important implications. AB splitting patterns in EPR spectra of biological systems with multiple paramagnetic centers are being recognized with increasing frequency.[10] The knowledge that exchange interaction can contribute to these splittings is crucial to a proper understanding of the geometry of the system. Electron transport occurs over relatively long distances via pathways that are poorly characterized. Understanding of the weak orbital overlaps that can be probed with electron–electron coupling constants may provide insight into the plausibility of proposed pathways.

Support of this work by grants from the NIH (GM21156) and the NSF (CHE78-16195 and CHE84-11282) is gratefully acknowledged. The names of our co-workers are included on the papers cited.